Citation for final published version:

Irimia, Marinela, Wang, Yu, Fei, Yifan, Knowles, Peter J. and Wang, Jian 2025. Band structure from the reduced density-matrix functional theory: application to Si and diamond [Letter]. Journal of Chemical Theory and Computation 10.1021/acs.jctc.5c01266

Publishers page: https://doi.org/10.1021/acs.jctc.5c01266

Band structure from the reduced density-matrix functional theory: application to Si and diamond

Marinela Irimia,[†] Yu Wang,[‡] Yifan Fei,[¶] Peter J. Knowles,[§] and Jian Wang[*,¶]

†*International School, Huzhou University, Zhejiang 313000, China*
‡*College of Mechanical Engineering, Jiaxing University, Zhejiang 314001, China*
¶*School of Science, Huzhou University, Zhejiang 313000, China*
§*School of Chemistry, Cardiff University, Main Building, Park Place, Cardiff CF10 3AT, United Kinddom*

E-mail: jwang572@hotmail.com

Abstract

The band structure from the reduced density-matrix functional theory with an entropic functional for correlation has a simple mathematical structure following the Fermi-Dirac distribution, which accommodates a band gap according to the occupation numbers of the lowest conduction band and the highest valence band. Calculations are demonstrated for Si and diamond with the exchange energy approximated using the X_α model.

A peculiar problem of density-functional theory (DFT) is the underestimates of band gaps for semiconductors and insulators, which has been argued to be persistent even with the unknown exact Kohn-Sham potential and is connected with the derivative discontinuity in the exchange-correlation energy.[1,2] It is not easy to design an exchange-correlation model with the correct derivative discontinuity, nevertheless, several sophisticated exchange-correlation functionals containing derivative discontinuity have been reported.[3–7] In recent years, several meta-generalized gradient approximation(GGA)[8–10] and hybrid functionals which mix some percentage of Hartree-Fock exchange with conventional exchange-correlation functionals,[11,12] have been found to improve the band gap, without the necessity to invoke derivative discontinuity.[13,14] In this paper, we study the band gap within the reduced density-matrix functional theory (RDMFT).[15,16]

In RDMFT, the variable is the one-particle reduced density-matrix (1RDM),

$$\gamma(1,1') = \sum_i^M n_i \chi_i(1)\chi_i^*(1') \tag{1}$$

where χ_i are called the natural orbitals,[17] and n_i are their occupation numbers. M is number of orbitals, which can be larger than the number of electrons N in the system. In the configuration interaction (CI) wave function method, electron correlation is brought in by adding more configurations, n_i is expressible through the expansion coefficients c_i of the configurations in wave function.[18]

The diagonal element $\gamma(1,1)$ is the density. The density in DFT is defined as

$$\rho(1) = \sum_i^N \varphi_i(1)\varphi_i^*(1) \tag{2}$$

where the orbitals φ_i, often called Kohn-Sham(KS) orbitals, are derived from the KS equations. The orbitals are occupied by the electrons according to the Aufbau principle. In case of no degeneracy at the Fermi level, only the lowest N orbitals from the total M orbitals are occupied by N electrons. The density in DFT is assumed to be identical to the density from the wave function, i.e. $\rho(1) = \gamma(1,1)$, so a density functional can be regarded as a density-matrix functional as well. In order to implement a density functional in the context of RDMFT, one need optimize both the orbitals $\chi_i(1)$ and their occupation numbers n_i.

The occupation number n_i in 1RDM follows the Pauli principle, i.e. $0 \leq n_i \leq 1$, which is also called the ensemble representability condition.[19] To comply with this condition, one usually changes variables by $n_i = \cos^2\theta_i$ so that the conditional variation problem is converted into a non-conditional variation problem. Gilbert then found that all partially occupied natural spin orbitals are degenerate, i.e. having the same orbital energy.[15] The consequence of this degeneracy is that one can not have a normal spectrum of orbital energies as one usually has with the Hartree-Fock equation or the KS equations in DFT. Burke[20] once commented that "if this methodology ever does become popular, it would represent a true paradigm shift, as it does not even use KS equations. But, for this reason, it is difficult to see how many of the impressive results of DFT approximations could be retained."

In our analysis of wave functions for small molecules, we observed a linear relation between the cumulant energy and the information entropy based on 1RDM.[21,22]

$$E_{\mathrm{cum}} = -\kappa S - b \tag{3}$$

Here κ and b are system dependent constants. Mazziotti *et al*[23] recently proposed an approximation for the cumulant energy based on the lowest unitary invariant of the cumulant, from which one may derive[24]

$$\kappa = \frac{2}{5M(M-1)} \sum_{i,j}^{M} \langle ij|ij\rangle - \langle ij|ji\rangle \tag{4}$$

where M is the total number of spin-orbitals, so κ is some average of the antisymmetrized two-electron integrals. Zamani and Carter-Fenk[25] recently proposed an alternative formula by connecting the cumulant energy to Mller-Plesset's second order perturbation energy. The constant b produces a shift to the whole energy surface, it can be used to set the reference zero energy.

For the information entropy S, its mathematical form may be different in classical or quantum theory. For fermions, it has the form,[26]

$$S = -\sum_i [n_i \ln n_i + (1 - n_i) \ln (1 - n_i)] \tag{5}$$

Justification for the entropic function has appeared in different contexts. Especially notable here is Weinert and Davenport 's discovery[27] that if fractional occupation numbers are allowed, then an additional term as Eq. (5) is required in the energy in order for it to be variational. The energy expression then looks like the free-energy in finite temperature DFT.[28,29] However, it is originated from fractional occupations, instead of temperature, so the entropy here is better identified as information entropy[30,31] or correlation entropy.[32] One consequence of the entropy term is the automatic removal of the extra force due to the changes in occupation number, which complicates force calculation in molecular dynamics simulation.[27,33] It also improves the description of static correlation and multi-reference property in DFT, which characterizes the CI method.[34]

Recently, we found that Gilbert's degeneracy problem in RDMFT can be removed with the entropic functional, so that self-consistent-field one-electron eigenvalue equation, as the Hartree-Fock equation or the KS equation in DFT, can be obtained.[35] Due to its connection to the information entropy, the method has been named as *i*-DMFT. It has since been successfully used to generate accurate potential energy curves as a result of total energy calculation.[24,36] In this paper, we focus on the band structure of solids.

In RDMFT, functionals are usually constructed based on an approximation to the two-particle reduced density-matrix (2RDM).[37–43] The 2RDM can be decomposed as[44,45]

$$\Gamma(1,2) = \frac{1}{2}[\gamma(1,1)\gamma(2,2) - \gamma(1,2)\gamma(2,1)] + \lambda(1,2). \tag{6}$$

The first term is the independent-particle contribution, the second term accounts for the exchange effect. The $\lambda(1,2)$ term is called the two-electron cumulant. The cumulant energy is defined as

$$E_{\text{cum}} = \int\int \frac{\lambda(1,2)}{r_{12}} d1d2 \tag{7}$$

which has been identified as the correlation energy in RDMFT by Levy.[46] The kinetic energy is expressed exactly with 1RDM, there is no need of a coupling-constant integration to fold any correction to the kinetic energy into the correlation energy as in DFT.[47] The modeling of correlation energy is more convenient in RDMFT, because its behavior can be checked against the cumulant energy from wave function calculations,[21,22] instead of relying on uniform electron gas model.

The exact exchange energy is

$$E_x = -\frac{1}{2}\int\int\frac{\gamma(1,2)\gamma(2,1)}{r_{12}}d1d2 \tag{8}$$

Unlike the exchange energy in DFT, the 1RDM $\gamma(1,2)$ here is non-idempotent. The difficulty to apply the exact exchange to solid systems is its long-range or nonlocal property.[48–50] For the similar problem in the Hartree-Fock method, Slater once proposed an approximation to the exchange potential and further simplified it to a density functional.[51] The idea led to the X_α model for E_x[52]

$$E_x[\rho(\mathbf{r})] = C_x\int\rho(\mathbf{r})^{4/3}d^3\mathbf{r} \tag{9}$$

$C_x = -(9/8)(3/\pi)^{1/3}\alpha$ in atomic unit. The parameter α can be optimized and is system dependent.[53,54] At the beginning, Slater proposed α=1, later the value $\alpha = 0.7$ becomes popular among X_α practitioners.[55,56] In DFT, the value α=2/3 is preferred and has been built into the exchange part of the local density approximation (LDA).[29] The choice of α=1 or 2/3 is due to different strategy in constructing the effective exchange potential, either taking the average or a state at the top of the Fermi distribution.[29,57] It is found that α=2/3 underestimates exchange energies[58] and the ionization energy (the negative orbital energy).[59,60] Verma and Truhlar[9,61] proposed the high local exchange (HLE) functional with a high α value, such as $\alpha = 1.25\times 2/3$, to improve semiconductor band gaps and excitation energies.

In the GGA model for exchange,[62,63] an enhancement factor $F_x(s)$ is introduced to systematically tune the exchange effect

$$E_x^{GGA}[\rho(\mathbf{r})] = \frac{2}{3}C_x \int \rho^{4/3} F_x(s) d^3\mathbf{r} \tag{10}$$

where s is a dimensionless density gradient. A similar enhancement factor is introduced in meta-GGA exchange model.[8,10] In the following, we will examine which exchange model is the most suitable to combine with the entropic correlation functional in band structure calculations.

The one-electron energies, including the kinetic energy and the electron-nucleus Coulomb energy, are expressed exactly with 1RDM, the total energy of an electronic system then becomes

$$\begin{aligned} E &= \sum_i h_{ii} n_i + \int\int \frac{\Gamma(1,2)}{r_{12}} d1d2 + Z \\ &= \sum_i h_{ii} n_i + \frac{1}{2}\sum_{ij} n_i n_j \langle ij|ij\rangle + E_x + E_{\text{cum}} + Z \end{aligned} \tag{11}$$

with $h_{ii} = \langle \chi_i|\hat{h}|\chi_i\rangle$ where

$$\hat{h} = -\frac{1}{2}\nabla_1^2 - \sum_\nu \frac{Z_\nu}{r_{1\nu}} \tag{12}$$

and $\langle ij|ij\rangle$ are the two-electron Coulomb integrals.[64] Z is the Coulomb interactions energy between all pairs of nuclei.

In RDMFT, the variables are $\{n_i\}$ and $\{\chi_i\}$. To optimize the energy E under the constraint $\sum n_i = N$ and the orthonormality conditions for the spin orbitals, one has the Lagrangean

$$\Omega = E - \mu\left(\sum_i n_i - N\right) - \sum_{ij} \lambda_{ij}[\langle \chi_i|\chi_j\rangle - \delta_{ij}] \tag{13}$$

where μ and λ_{ij} are Lagrange multipliers. Using the chain rule with $\rho(1) = \sum_i n_i \chi_i(1)\chi_i^*(1)$

$$\frac{\partial E_x[\rho(1)]}{\partial \chi_i^*(1)} = \frac{\delta E_x[\rho(1)]}{\delta \rho(1)} \frac{\partial \rho(1)}{\partial \chi_i^*(1)} \tag{14}$$

the Euler-Lagrange equations $\partial\Omega/\partial\chi_i^*(1) = 0$ yield

$$n_i[\hat{h} + \sum_j n_j \hat{J}_j + V_x]\chi_i(1) = \sum_k \lambda_{ik}\chi_k(1) \tag{15}$$

where $V_x = \delta E_x[\rho(1)]/\delta\rho(1)$.

The Hermitian property of Lagrange multipliers λ_{ki} requires $\lambda_{ik} = \lambda_{ki}^*$, i.e. $(n_i - n_k)\langle k|\hat{f}|i\rangle = 0$, which implies an eigenvalue problem for the orbitals

$$\hat{f}\chi_i(1) = \epsilon_i\chi_i(1) \tag{16}$$

where the operator $\hat{f}$ is,

$$\hat{f} = \hat{h} + \sum_j n_j \hat{J}_j + V_x \tag{17}$$

The Euler-Lagrange equations $\partial\Omega/\partial n_i = 0$ for the occupation numbers yield

$$h_{ii} + \sum_j n_j \langle ij|ij\rangle + \langle i|V_x|i\rangle + \kappa[\ln n_i - \ln(1 - n_i)] = \mu \tag{18}$$

Once the eigenvalue Eq. (16) is solved, we insert the eigenvalues ϵ_i into the above equation to obtain

$$\epsilon_i + \kappa[\ln n_i - \ln(1 - n_i)] = \mu \tag{19}$$

which leads to the solution

$$n_i = \frac{1}{1 + \exp[(\epsilon_i - \mu)/\kappa]} \tag{20}$$

Thus the occupation numbers follow the Fermi-Dirac distribution, which automatically satisfy the ensemble representability conditions. The Lagrange multiplier μ is fixed by the sum rule $\sum n_i = N$.

Previously, the Fermi-Dirac distribution is invoked as an *ad hoc* convenience to accelerate convergence.[65,66] In this method, the Fermi-Dirac distribution is intrinsic, so the calculation converges fast.

The calculation of band gap in DFT is connected with Janak's theorem,[67]

$$\partial E/\partial n_i = \epsilon_i \tag{21}$$

i.e. the orbital energy is equal to the derivative of the total energy with respect to the orbital occupation. The result is independent of the exchange-correlation functional. Similar relation has been known in Hartree-Fock and X_α method.[68] Janak's theorem is based on fractional variable occupation numbers, as Weinert and Davenport pointed out,[27] fractional occupation numbers should come along with an entropic term. In our case,

$$\frac{\partial E}{\partial n_i} = \epsilon_i + \kappa[\ln n_i - \ln(1-n_i)] \tag{22}$$

Janak noted that when an electron is added to or removed from an infinite periodic solid, the highest occupied orbital energy will change only infinitesimally. Due to $\int_0^1[\ln f - \ln(1-f)]df$=0, the following important relations discussed by Perdew *et al*[1,69,70] still hold

$$\begin{aligned} I(N) = E(N-1) - E(N) &= -\int_0^1 \epsilon_N(N-1+f)df = -\epsilon_N(N-\delta) \\ A(N) = E(N) - E(N+1) &= -\int_0^1 \epsilon_{N+1}(N+f)df = -\epsilon_{N+1}(N+\delta) \end{aligned} \tag{23}$$

where δ is a positive infinitesimal, $I(N)$ is the ionization potential and $A(N)$ is the electron affinity of a N-electron system. $\epsilon_N(N)$ and $\epsilon_{N+1}(N)$ are, respectively, the highest valence band and the lowest conduction band of the N-electron system. As electron number increases through an integer N, the chemical potential jumps from $E(N) - E(N-1)$ to $E(N+1) - E(N)$, the band gap or fundamental band gap can be written as.[1,2]

$$E_g = I(N) - A(N) = \epsilon_{N+1}(N) - \epsilon_N(N) + C \tag{24}$$

where C is the derivative discontinuity caused by the exchange-correlation energy. For exchange-correlation functional which is continuous, such as LDA, X$_\alpha$, etc., then C=0.[13]

In solids, orbitals take the Bloch form $\chi_{i,\mathbf{k}} = \exp^{-i\mathbf{k}\cdot\mathbf{r}} u_{i,\mathbf{k}}$, where the subscript i is for band index and $\mathbf{k}$ is for the k-point vector in the Brillouin zone.[71] For practical calculations, we choose the CP2K package which is an open source code.[72] The equations to solve the orbitals and occupation numbers can be realized with the smearing technique using the Fermi-Dirac scheme.[73] For the band structure of Si and diamond, we choose the DZVP basis set and GTH pseudopotentials,[74] along with the $8 \times 8 \times 8$ Monkhorst-Pack[75] set of k-points to sample the Brillouin zone.

In this paper, we take a pragmatic approach to determine the parameters in the entropic functional for correlation and the X$_\alpha$ model for exchange. For the parameter b in Eq. (3), it amounts to shifting the whole potential energy surface with a constant. Its value does not affect the identification of the minimum from the total energy calculations, and also the eigenvalue equation Eq. (16) does not dependent on b, so it can be set to zero. Start with an initial value, say α=2/3 for the X$_\alpha$ model, κ will be optimized until the minimum of the potential energy surface locates at the experimental lattice constant. Then the band structure is calculated and the band gap is identified. If the band gap does not equal to the experimental band gap within a given accuracy (say 0.001 eV), the parameter α is then modified and above computation steps are repeated.

Table 1 displays test results for Si, along with the experimental data and the LDA result. The message from the Table 1 is that all exchange-only models, LDA$_x$, GGA$_x$, and meta-GGA$_x$, give equilibrium lattice constants larger than the experimental lattice constant. LDA$_x$ gives R_e=5.527Å. GGA$_x$ gives R_e=5.696Å, even larger than LDA$_x$. That is unexpected because the GGA$_x$ model has an enhancement factor $F_x(s) \geq 1$. When we look carefully at the total energy data, there are too many spurious minima, that is caused by the oscillating behavior of $F_x(s)$. Similar behavior has

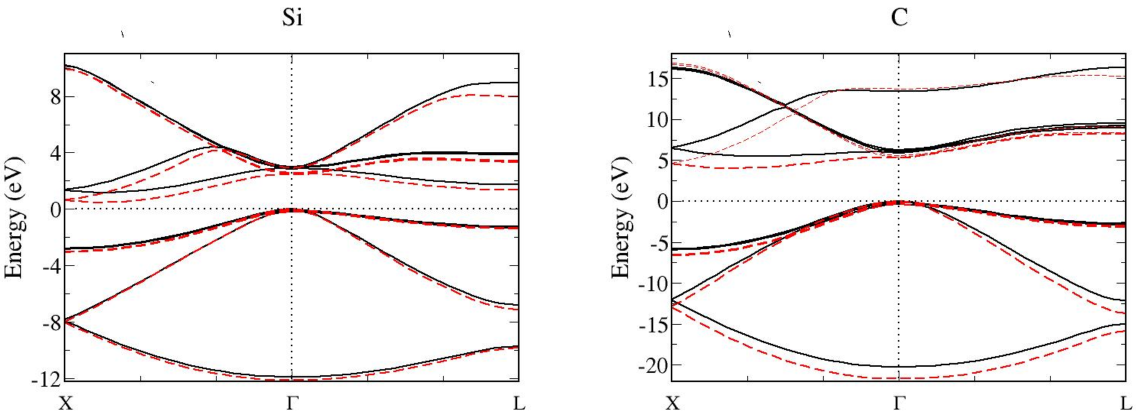

Figure 1: Band structure of Si and diamond in this work (black) compared to LDA (dashed red). For Si, the exchange-correlation functional is $X_{\alpha=24/25}$ + $E_{\text{cum}}(\kappa = 26520)$, which gives a lattice constant 5.43 Å and band gap 1.17 eV. For diamond, the exchange-correlation functional is $X_{\alpha=1.24}$ + $E_{\text{cum}}(\kappa = 61920)$. which gives a lattice constant 3.567 Å and band gap 5.48 eV.

Table 1: The lattice constant R_e and the indirect band gap E_g for Si from different computational methods, compared to the experimental data.

	R_e (Å)	E_g (eV)
Expt.	5.430	1.17
LDA	5.433	0.47
LDA$_x$($X_{\alpha=2/3}$)	5.527	0.43
GGA$_x$ (PW86[62])	5.696	0.57
meta-GGA$_x$ (SCAN[8])	5.556	1.51
$X_{\alpha=1}$	5.053	0.74
$X_{\alpha=1}$ + $E_{\text{cum}}(\kappa$=29000)	5.430	1.26
$X_{\alpha=24/25}$ + $E_{\text{cum}}(\kappa$=26520)	5.430	1.17

Table 2: The lattice constant R_e and the indirect band gap E_g for diamond from different parameters of α and κ, compared to experimental data and LDA calculation.

	R_e (Å)	E_g (eV)
Expt.	3.567	5.48
LDA	3.542	4.02
$X_{\alpha=0.8}$ + $E_{\text{cum}}(\kappa$=30000)	3.567	4.31
$X_{\alpha=0.9}$ + $E_{\text{cum}}(\kappa$=38700)	3.567	4.60
$X_{\alpha=1.0}$ + $E_{\text{cum}}(\kappa$=46050)	3.567	4.87
$X_{\alpha=1.1}$ + $E_{\text{cum}}(\kappa$=52880)	3.567	5.13
$X_{\alpha=1.2}$ + $E_{\text{cum}}(\kappa$=59370)	3.567	5.38
$X_{\alpha=1.24}$ + $E_{\text{cum}}(\kappa$=61920)	3.567	5.48

Table 3: The band energies in Si at special k-points Γ, X and L from present calculations and compared with available theoretical and experimental data. Energies are given in eV and measured with respect to the valence-band maximum (Γ'_{25v}).

k-point	LDA[76]	LDA	$X_{\alpha=24/25} + E_{\text{cum}}$	GW[77]	Expt.[77]
Γ_{1v}	-11.93	-12.12	-11.90	12.04	-12.5
Γ'_{25v}	0	0	0	0	0
Γ_{15c}	2.53	2.44,2.56	2.84,2.96	3.35	3.4
Γ'_{2c}	3.29	2.90	2.98	4.08	4.2
X_{1v}	-7.78	-7.98,-8.07	-7,86,-7.94		-7.94
X_{4v}	-2.88	-3.00,-3.05	-2.77,-2.82	-2.99	-2.9,-3.3
X_{1c}	0.61	0.59,0.65	1.31,1.38	1.44	1.3
X_{3c}	9.97	9.97	10.14		
L'_{2v}	-9.52	-9.85	-9.73	-9.79	-9.3
L_{1v}	-7.00	-7.12	-6.8	-7.18	
L'_{3v}	-1.20	-1.33,-1.40	-1.25,-1.32	-1.27	-1.2,-1.5
L_{1c}	1.48	1.34	1.72	2.27	2.1,2.4
L_{3c}	3.31	3.33,3.42	3.85,3.94	4.24	4.15
L'_{2c}	7.48	7.97	8.90		

been reported in functionals employing gradient.[52,78,79] The meta-GGA$_x$ model of SCAN[8] does not show oscillating behavior in total energy, it gives a single minimum at R_e=5.556 Å. A remarkable difference of the $X_{\alpha=1}$ model from LDA$_x$, GGA$_x$ and meta-GGA$_x$ is the shrinkage of the lattice constant R_e=5.053 Å, which is less than the experimental value of 5.430 Å.

The correlation functional in DFT are orbital or density dependent, which can reduce the lattice constant, as is evident from comparison of the lattice constants from LDA$_x$ and LDA. However, the entropic functional in RDMFT is only occupation-number dependent. The mathematic form of the entropic functional also appears in finite temperature formulation of DFT,[28,29] κ reflects the effect of temperature. Increasing κ tends to populate electrons into higher virtual orbitals, which will eventually cause the lattice constant to expand. Since the lattice constant from LDA$_x$, or GGA$_x$, or meta-GGA$_x$ is larger than the experimental value, it is no more possible to reduce the lattice constant to the experimental value of 5.430 Å with the entropic functional. But it is different if we combine the entropic functional with the $X_{\alpha=1}$ model. By increase the parameter κ to 29000 K, we arrive at a lattice constant equal to the experimental value of 5.430 Å. The lattice gives a band gap E_g=1.26 eV, which agrees well with the value E_g=1.29 eV[77] or E_g=1.24[80] predicted by two separate *GW* calculations.

For Si, one can still tune the two parameters, α for exchange and κ for correlation, to find the best values for the lattice constant and the band gap, i.e. $\alpha = 24/25 =$ and κ=26520 K. The band structure is displayed in Fig. 1 along with that from LDA (dashed red). A remarkable feature is the up-shift of the conduction bands from the corresponding LDA bands.

Similar calculation for diamond is shown in Table 2. The band structure is compared with the LDA result (in red) also in Fig. 1. Diamond has a large band gap at 5.48 eV, a large κ is expected to excite electron to the higher virtual orbitals. A large $\alpha \geq 1$ has been previously reported for molecules.[54] For a given α value, κ can be varied to fit the lattice constant to the experimental value, then the band structure can be calculated and band gap deducted. The procedures is repeated until both the experimental lattice constant and band gap are reproduced. For diamond, it occurs at α=1.24 and κ=61920 K. The *GW* band gap for diamond is E_g=5.6 eV[77] or E_g=5.33[80] from two separate groups.

From Eq. (19) or the Fermi-Dirac distribution of Eq. (20), by eliminating μ, one obtains a simple formula for the energy difference of any two levels

$$\epsilon_1 - \epsilon_2 = \kappa\{\ln[n_2(1 - n_1)] - \ln[n_1(1 - n_2)]\} \tag{25}$$

In RDMFT, the valence bands are those with occupation number close to 1, while the conduction bands are those close to 0. If n_1 is the highest valance band and n_2 is the lowest conduction band, then because the logarithmic function rises sharply for an argument between 0 and 1, $\ln[n_2(1 - n_1)] - \ln[n_1(1 - n_2)]$ gives rise to a large factor, which is the reason for the opening up of the band gap.

The band energies at special points for Si are listed in Table 3. For comparison, the theoretical LDA calculation by Yin and Cohen,[76] *GW* calculation by Hybertsen and Louie[77] and the experimental data[77] are also listed. The slight difference in our LDA data from Yin and Cohen's[76] can be due to different pseudopotentials employed in the calculations. Their data of lattice constant

R_e=5.451 Å and band gap E_g=0.48 eV agree well with our LDA data. In some entry of the Table 3, there are two numbers, that is due to lifting of degeneracy. Fig. 1 and Table 3 indicate that the band structure from RMDFT is comparable to available theoretical and experimental results.

In conclusion, band structure is realized for the first time in 50 years since Gilbert's first RDMFT paper.[15] The method is based on a correlation functional measured by the information entropy (*i*-DMFT[35]). Unlike DFT orbital or density dependent correlation functional, the occupation-number dependent entropic functional has a tendency to stretch the lattice constant. To combine with the entropic functional, the X_α model for exchange is more convenient to adjust than conventional DFT exchange models. The band structure follows the Fermi-Dirac distribution, so the band gap can be written in closed form in terms of orbital occupation numbers and a system dependent parameter κ, as shown in Eq. (25). The two parameters, α for exchange and κ for correlation, can be optimized by explicit try-and-error calculations to reproduce the lattice constant and band gap, as demonstrated for Si and diamond. Lattice constants are usually available from X-ray diffraction. If experimental band gap is not available, one may choose other data such as excitation energy, ionization energy, etc. to fit the parameters. The method can be implemented within current DFT softwares coded with the Fermi-Dirac smearing technique, and provides an efficient alternative to DFT method for band structure.

Acknowledgement

Financial support from the Zhejiang National Science Foundation (LY23A040003) and China National Science Foundation (12574063) is acknowledged.

References

(1) Perdew, J. P.; Levy, M. Physical Content of the Exact Kohn-Sham Orbital Energies: Band Gaps and Derivative Discontinuities. *Phys. Rev. Lett.* **1983**, *51*, 1884–1887.

(2) Sham, L. J.; Schlüter, M. Density-Functional Theory of the Energy Gap. *Phys. Rev. Lett.* **1983**, *51*, 1888–1891.

(3) Städele, M.; Majewski, J. A.; Vogl, P.; Görling, A. Exact Kohn-Sham Exchange Potential in Semiconductors. *Phys. Rev. Lett.* **1997**, *79*, 2089–2092.

(4) Tran, F.; Blaha, P. Accurate Band Gaps of Semiconductors and Insulators with a Semilocal Exchange-Correlation Potential. *Phys. Rev. Lett.* **2009**, *102*, 226401.

(5) Kuisma, M.; Ojanen, J.; Enkovaara, J.; Rantala, T. T. Kohn-Sham potential with discontinuity for band gap materials. *Phys. Rev. B* **2010**, *82*, 115106.

(6) Armiento, R.; Kümmel, S. Orbital Localization, Charge Transfer, and Band Gaps in Semilocal Density-Functional Theory. *Phys. Rev. Lett.* **2013**, *111*, 036402.

(7) Eich, F. G.; Hellgren, M. Derivative discontinuity and exchange-correlation potential of meta-GGAs in density-functional theory. *J. Chem. Phys.* **2014**, *141*, 224107.

(8) Sun, J.; Ruzsinszky, A.; Perdew, J. P. Strongly Constrained and Appropriately Normed Semilocal Density Functional. *Phys. Rev. Lett.* **2015**, *115*, 036402.

(9) Verma, P.; Truhlar, D. G. HLE17: An Improved Local Exchange–Correlation Functional for Computing Semiconductor Band Gaps and Molecular Excitation Energies. *J. Phys. Chem. C* **2017**, *121*, 7144–7154.

(10) Lebeda, T.; Aschebrock, T.; Kümmel, S. Balancing the Contributions to the Gradient Expansion: Accurate Binding and Band Gaps with a Nonempirical Meta-GGA. *Phys. Rev. Lett.* **2024**, *133*, 136402.

(11) Krukau, A. V.; Vydrov, O. A.; Izmaylov, A. F.; Scuseria, G. E. Influence of the exchange screening parameter on the performance of screened hybrid functionals. *J. Chem. Phys.* **2006**, *125*, 224106.

(12) Wang, Y.; Verma, P.; Zhang, L.; Li, Y.; Liu, Z.; Truhlar, D. G.; He, X. M06-SX screened-exchange density functional for chemistry and solid-state physics. *PNAS* **2020**, *117*, 2294–2301.

(13) Perdew, J. P.; Yang, W.; Burke, K.; Yang, Z.; Gross, E. K. U.; Scheffler, M.; Scuseria, G. E.; Henderson, T. M.; Zhang, I. Y.; Ruzsinszky, A.; Peng, H.; Sun, J.; Trushin, E.; Görling, A. Understanding band gaps of solids in generalized Kohn–Sham theory. *PNAS* **2017**, *114*, 2801–2806.

(14) Perdew, J. P.; Ruzsinszky, A. Density-functional energy gaps of solids demystified. *European Phys. J. B* **2018**, *91*, 108.

(15) Gilbert, T. Hohenberg-Kohn theorem for nonlocal external potentials. *Phys. Rev. B* **1975**, *12*, 2111–2120.

(16) Levy, M. Universal variational functionals of electron densities, first-order density matrices, and natural spin-orbitals and solution of the v-representability problem. *Proc. Natl. Acad. Sci. U.S.A.* **1979**, *76*, 6062–6065.

(17) Löwdin, P.-O. Quantum Theory of Many-Particle Systems. I. Physical Interpretations by Means of Density Matrices, Natural Spin-Orbitals, and Convergence Problems in the Method of Configurational Interaction. *Phys. Rev.* **1955**, *97*, 1474–1489.

(18) Wang, Y.; Wang, J.; Lischka, H. Lagrange function method for energy optimization directly in the space of natural orbitals. *Int. J. Quantum Chem.* **2017**, *117*, e25376.

(19) Coleman, A. J. Structure of Fermion Density Matrices. *Rev. Mod. Phys.* **1963**, *35*, 668–686.

(20) Burke, K. Perspective on density functional theory. *J. Chem. Phys.* **2012**, *136*, 150901.

(21) Wang, Y.; Knowles, P. J.; Wang, J. Information entropy as a measure of the correlation energy associated with the cumulant. *Phys. Rev. A* **2021**, *103*, 062808.

(22) Irimia, M.; Wang, Y.; Fei, Y.; Wang, J. Self-consistent-field method for correlation calculation within density-matrix-functional theory. *Phys. Rev. A* **2023**, *108*, 052818.

(23) Gibney, D.; Boyn, J.-N.; Mazziotti, D. A. Universal Generalization of Density Functional Theory for Static Correlation. *Phys. Rev. Lett.* **2023**, *131*, 243003.

(24) Liu, D.; Irimia, M.; Wang, J.; Yan, B. Potential Energy Curves of Hydrogen Halides HX(F, Cl, Br) with the i-DMFT Method. *J. Phys. Chem. A* **2025**, *129*, 415–422.

(25) Zamani, A. Y.; Carter-Fenk, K. Toward ab initio realizations of Collins's conjecture. *J. Chem. Phys.* **2025**, *163*, 034103.

(26) Landau, L.; Lifshitz, E. *Statistical Physics*; Pergamon Press: London, 1958.

(27) Weinert, M.; Davenport, J. W. Fractional occupations and density-functional energies and forces. *Phys. Rev. B* **1992**, *45*, 13709–13712.

(28) Mermin, N. D. Thermal Properties of the Inhomogeneous Electron Gas. *Phys. Rev.* **1965**, *137*, A1441–A1443.

(29) Kohn, W.; Sham, L. J. Self-Consistent Equations Including Exchange and Correlation Effects. *Phys. Rev.* **1965**, *140*, A1133–A1138.

(30) Collins, D. M. Entropy maximizations on electron density. *Z. Naturforsch* **1993**, *48a*, 68–74.

(31) Jaynes, E. T. Information Theory and Statistical Mechanics. II. *Phys. Rev.* **1957**, *108*, 171–190.

(32) Gersdorf, P.; John, W.; Perdew, J. P.; Ziesche, P. Correlation entropy of the H2 molecule. *Int. J. Quantum Chem.* **1997**, *61*, 935–941.

(33) Wentzcovitch, R. M.; Martins, J. L.; Allen, P. B. Energy versus free-energy conservation in first-principles molecular dynamics. *Phys. Rev. B* **1992**, *45*, 11372–11374.

(34) Chai, J.-D. Density functional theory with fractional orbital occupations. *J. Chem. Phys.* **2012**, *136*, 154104.

(35) Wang, J.; Baerends, E. J. Self-Consistent-Field Method for Correlated Many-Electron Systems with an Entropic Cumulant Energy. *Phys. Rev. Lett.* **2022**, *128*, 013001.

(36) Liu, D.; Yan, B.; Irimia, M.; Wang, J. Potential energy curves for F2, Cl2, and Br2 with the i-DMFT method. *J. Chem. Phys.* **2024**, *161*, 044118.

(37) Müller, A. M. K. Explicit approximate relation between reduced two- and one-particle density matrices. *Phys. Lett. A* **1984**, *105*, 446–452.

(38) Goedecker, S.; Umrigar, C. J. Natural Orbital Functional for the Many-Electron Problem. *Phys. Rev. Lett.* **1998**, *81*, 866–869.

(39) Yasuda, K. Local Approximation of the Correlation Energy Functional in the Density Matrix Functional Theory. *Phys. Rev. Lett.* **2002**, *88*, 053001.

(40) Staroverov, V. N.; Scuseria, G. E. Assessment of simple exchange-correlation energy functionals of the one-particle density matrix. *J. Chem. Phys.* **2002**, *117*, 2489–2495.

(41) Rohr, D. R.; Pernal, K.; Gritsenko, O. V.; Baerends, E. J. A density matrix functional with occupation number driven treatment of dynamical and nondynamical correlation. *J. Chem. Phys.* **2008**, *129*, 164105.

(42) Sharma, S.; Dewhurst, J. K.; Shallcross, S.; Gross, E. K. U. Spectral Density and Metal-Insulator Phase Transition in Mott Insulators within Reduced Density Matrix Functional Theory. *Phys. Rev. Lett.* **2013**, *110*, 116403.

(43) Piris, M. Global Natural Orbital Functional: Towards the Complete Description of the Electron Correlation. *Phys. Rev. Lett.* **2021**, *127*, 233001.

(44) Mazziotti, D. A. Approximate solution for electron correlation through the use of Schwinger probes. *Chem. Phys. Lett.* **1998**, *289*, 419–427.

(45) Kutzelnigg, W.; Mukherjee, D. Cumulant expansion of the reduced density matrices. *J. Chem. Phys.* **1999**, *110*, 2800–2809.

(46) Levy, M. Correlation Energy Functionals of One-Matrices and Hartree-Fock Densities. Density Matrices and Density Functionals. Dordrecht, 1987; pp 479–498.

(47) Levy, M. Elementary Concepts in Density Functional Theory. *Theoret. Comput. Chem.* **1996**, *4*, 3–24.

(48) Duchemin, I.; Gygi, F. A scalable and accurate algorithm for the computation of Hartree–Fock exchange. *Comput. Phys. Comm.* **2010**, *181*, 855–860.

(49) Lin, P.; Ren, X.; He, L. Efficient Hybrid Density Functional Calculations for Large Periodic Systems Using Numerical Atomic Orbitals. *J. Chem. Theory Comput.* **2021**, *17*, 222–239.

(50) Bussy, A.; Hutter, J. Efficient periodic resolution-of-the-identity Hartree–Fock exchange method with k-point sampling and Gaussian basis sets. *J. Chem. Phys.* **2024**, *160*, 064116.

(51) Slater, J. C. A Simplification of the Hartree-Fock Method. *Phys. Rev.* **1951**, *81*, 385–390.

(52) Slater, J. C.; Wood, J. H. Statistical exchange and the total energy of a crystal. *Inter. J. Quant. Chem.* **1970**, *5*, 3–34.

(53) Schwarz, K. Optimization of the Statistical Exchange Parameter α for the Free Atoms H through Nb. *Phys. Rev. B* **1972**, *5*, 2466–2468.

(54) Zope, R. R.; Dunlap, B. I. Slater's Exchange Parameters α for Analytic and Variational Xα Calculations. *J. Chem. Theory Comput.* **2005**, *1*, 1193–1200.

(55) Baerends, E.; Ros, P. Self-consistent molecular Hartree—Fock—Slater calculations II. The effect of exchange scaling in some small molecules. *Chem. Phys.* **1973**, *2*, 52–59.

(56) Dunlap, B. I.; Connolly, J. W. D.; Sabin, J. R. On first-row diatomic molecules and local density models. *J. Chem. Phys.* **1979**, *71*, 4993–4999.

(57) Slater, J. C. The self-consistent field for crystals. *Inter. J. Quant. Chem.* **1969**, *4*, 727–746.

(58) Tong, B. Y.; Sham, L. J. Application of a Self-Consistent Scheme Including Exchange and Correlation Effects to Atoms. *Phys. Rev.* **1966**, *144*, 1–4.

(59) Gritsenko, O. V.; Mentel, L. M.; Baerends, E. J. On the errors of local density (LDA) and generalized gradient (GGA) approximations to the Kohn-Sham potential and orbital energies. *J. Chem. Phys.* **2016**, *144*, 204114.

(60) Baerends, E. J. Density functional approximations for orbital energies and total energies of molecules and solids. *J. Chem. Phys.* **2018**, *149*, 054105.

(61) Verma, P.; Truhlar, D. G. HLE16: A Local Kohn–Sham Gradient Approximation with Good Performance for Semiconductor Band Gaps and Molecular Excitation Energies. *J. Phys. Chem. Lett.* **2017**, *8*, 380–387.

(62) Perdew, J. P.; Yue, W. Accurate and simple density functional for the electronic exchange energy: Generalized gradient approximation. *Phys. Rev. B* **1986**, *33*, 8800–8802.

(63) Perdew, J. P.; Burke, K.; Ernzerhof, M. Generalized Gradient Approximation Made Simple. *Phys. Rev. Lett.* **1996**, *77*, 3865–3868.

(64) Szabo, A.; Ostlund, N. *Modern Quantum Chemistry: Introduction to Advanced Electronic Structure Theory*; Dover Pubs.: Dover US, 1996.

(65) Goedecker, S. Linear scaling electronic structure methods. *Rev. Mod. Phys.* **1999**, *71*, 1085–1123.

(66) Rabuck, A. D.; Scuseria, G. E. Improving self-consistent field convergence by varying occupation numbers. *J. Chem. Phys.* **1999**, *110*, 695–700.

(67) Janak, J. F. Proof that $\frac{\partial E}{\partial n_i} = \epsilon$ in density-functional theory. *Phys. Rev. B* **1978**, *18*, 7165–7168.

(68) Slater, J. C. In *Statistical Exchange-Correlation in the Self-Consistent Field*; Löwdin, P.-O., Ed.; Adv. Quant. Chem.; Academic Press, 1972; Vol. 6; pp 1–92.

(69) Perdew, J. P.; Parr, R. G.; Levy, M.; Balduz, J. L. Density-Functional Theory for Fractional Particle Number: Derivative Discontinuities of the Energy. *Phys. Rev. Lett.* **1982**, *49*, 1691–1694.

(70) Perdew, J. P. In *Density Functional Methods In Physics*; Dreizler, R. M., da Providência, J., Eds.; Springer US: Boston, MA, 1985; pp 265–308.

(71) Wang, J.; Wang, Y.; Yu, S.; Kolb, D. Nonlinear algorithm for the solution of the Kohn–Sham equations in solids. *Journal of Physics: Condensed Matter* **2005**, *17*, 3701.

(72) Kühne, T. D. et al. CP2K: An electronic structure and molecular dynamics software package - Quickstep: Efficient and accurate electronic structure calculations. *J. Chem. Phys.* **2020**, *152*, 194103.

(73) Kresse, G.; Furthmüller, J. Efficient iterative schemes for ab initio total-energy calculations using a plane-wave basis set. *Phys. Rev. B* **1996**, *54*, 11169–11186.

(74) Goedecker, S.; Teter, M.; Hutter, J. Separable dual-space Gaussian pseudopotentials. *Phys. Rev. B* **1996**, *54*, 1703–1710.

(75) Monkhorst, H. J.; Pack, J. D. Special points for Brillouin-zone integrations. *Phys. Rev. B* **1976**, *13*, 5188–5192.

(76) Yin, M. T.; Cohen, M. L. Theory of static structural properties, crystal stability, and phase transformations: Application to Si and Ge. *Phys. Rev. B* **1982**, *26*, 5668–5687.

(77) Hybertsen, M. S.; Louie, S. G. Electron correlation in semiconductors and insulators: Band gaps and quasiparticle energies. *Phys. Rev. B* **1986**, *34*, 5390–5413.

(78) Johnson, E. R.; Becke, A. D.; Sherrill, C. D.; DiLabio, G. A. Oscillations in meta-generalized-gradient approximation potential energy surfaces for dispersion-bound complexes. *J. Chem. Phys.* **2009**, *131*, 034111.

(79) Lehtola, S.; Marques, M. A. L. Many recent density functionals are numerically ill-behaved. *J. Chem. Phys.* **2022**, *157*, 174114.

(80) Godby, R. W.; Schlüter, M.; Sham, L. J. Accurate Exchange-Correlation Potential for Silicon and Its Discontinuity on Addition of an Electron. *Phys. Rev. Lett.* **1986**, *56*, 2415–2418.

TOC Graphic